

CENTRO INTERNAZIONALE
DI SCIENZE MECCANICHE

INTERNATIONAL CENTRE
FOR MECHANICAL SCIENCES

I-33100 UDINE (Italy), Palazzo del Torso, Piazza Garibaldi, 18

CONTRIBUTION OF PHOTOGRAMMETRY TO THE CONTROL OF DISPLACEMENTS

Dieter Fritsch
Chair of Photogrammetry
Technical University of Munich
Arcisstrasse 21
D-8000 Munich 2
Federal Republic of Germany

Paper presented to the course "Progettazione e ottimizzazione del rilievo topografico e fotogrammetrico di controllo", March 7-8, 1988

CONTRIBUTION OF PHOTOGRAMMETRY TO THE CONTROL OF DISPLACEMENTS *

Dieter Fritsch, Chair of Photogrammetry, Technical University of Munich, Arcisstrasse 21, D-8000 Munich 2, Federal Republic of Germany

Summary

The progress in photogrammetry in the recent past extended the applications from purely mapping in the beginning to precise point determination and object reconstruction. Today photogrammetric science is concentrated on digital photogrammetry to provide for real-time systems, which make photogrammetry still more attractive. Besides measurement systems depending only on photogrammetric methods, there is also a trend to integrate vision sensors into electronic theodolites leading to a new generation of surveying equipment.

For that reason the paper reviews at first the developments in analytical photogrammetry. Based on the concepts of bundle block adjustment some models and hypothesis tests are introduced to monitor displacements and to control the shape of industrial objects. But following the trend especially in close range applications also possibilities of an automated data flow from data capturing to object reconstruction are exhibited to demonstrate the full potential of future photogrammetric systems. Some examples cover accuracies and the efficiency of modern photogrammetry.

1. Introduction

The application of photogrammetry - the science of image metrology and image understanding - dates back more than hundred years. Although it was primarily used for a long time in medium scale topographic mapping, the introduction of digital computing power extended the application fields considerably. Nowadays photogrammetry provides also for large scale mapping in architecture, precise point determination in cadastre and engineering projects as well as for object descriptions by means of surface models. Most recently it is searching for new tasks in robotics and machine vision.

These developments were made possible by solving the image / object space relations analytically. Already towards the middle of the fifties H.H. Schmid (1956) introduced the concept of bundle block adjustment, which has been integrated into modern strategies of statistical inference during the last decade. At the same time U.V. Helava (1957) gave first considerations on a new generation of evaluation instruments - the analytical plotter (AP) - nowadays mostly used and generalized to photogrammetric information systems.

Although analytical photogrammetry has reached a high performance in accuracy and efficiency the progress in microelectronics and semiconductor technology influences photogrammetry once more. With the use of digital image sensors the photogrammetric data acquisition process can

totally be revised. This means, that all the operations from data capturing to object reconstruction may be done in "real-time" leading to the concept of "real-time photogrammetry". Especially in close range applications digital photogrammetric methods will considerably contribute to the discipline of "computer vision", as it is used nowadays in robotics and machine vision applications. Also the analytical plotter will be substituted by hard- and software used in these applications resulting into "digital plotters (DP)" as specific picture processing systems.

2. Analytical Photogrammetry in General

In order to extract informations from pictures taken at aerial positions (aerial photogrammetry) or on the earth (terrestrial photogrammetry) some definitions and explanations must be introduced. A look at the data flow (see Fig. 1) demonstrates the steps necessary to describe an object by means of photogrammetry

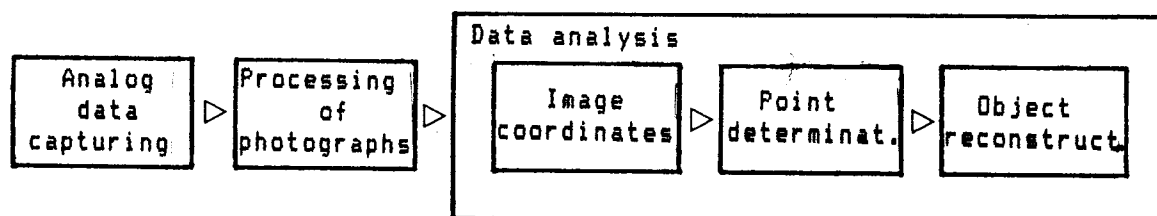


Fig. 1: Data flow in photogrammetry

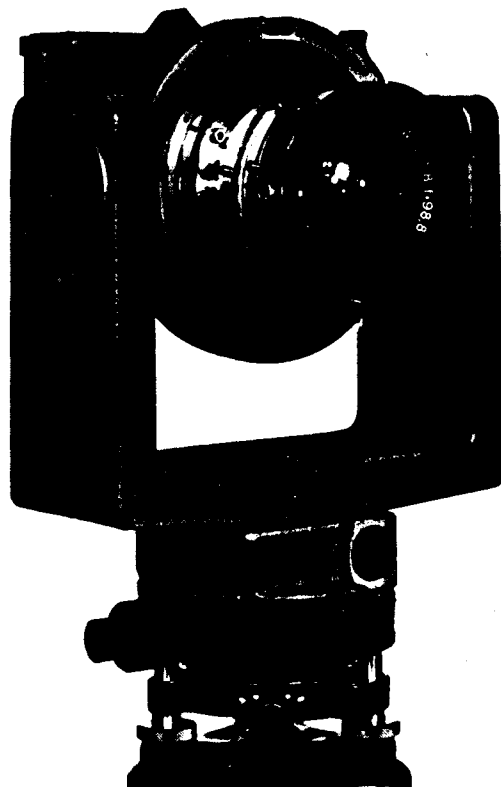
- (i) Data capturing can be done using metric cameras or professional amateur cameras. In the recent past some amateur cameras have been investigated (W. Wester-Ebbinghaus, 1983, M. Stephani/K. Eder, 1987) and recommended especially for close range applications. Typical examples for a metric and a semi-metric (amateur) camera are given by Fig. 2a, b.
- (ii) The processing step contains the procedures to obtain the final photograph from the exposed emulsion.
- (iii) Data analysis may be subdivided into three parts:
 - (1) the measurement of image coordinates by means of a monocomparator or an analytical plotter (see Fig. 2c)
 - (2) solving the collinearity equations between the image / object space for the unknown orientation parameters of the camera positions and the unknown spatial coordinates of the object points
 - (3) to describe the object point manifold by means of heuristic or analytical models. Especially in close range applications analytical model building is often desired to prove the quality of industrial objects and to parameterize architectural buildings, respectively. Also in deformation analysis this approach is used to model movements of points observed at different time epochs. On the contrary complex structures such as the earth

surface or car bodies in industry are represented by digital surface (terrain) models using grids and/or triangles as geometric cells.

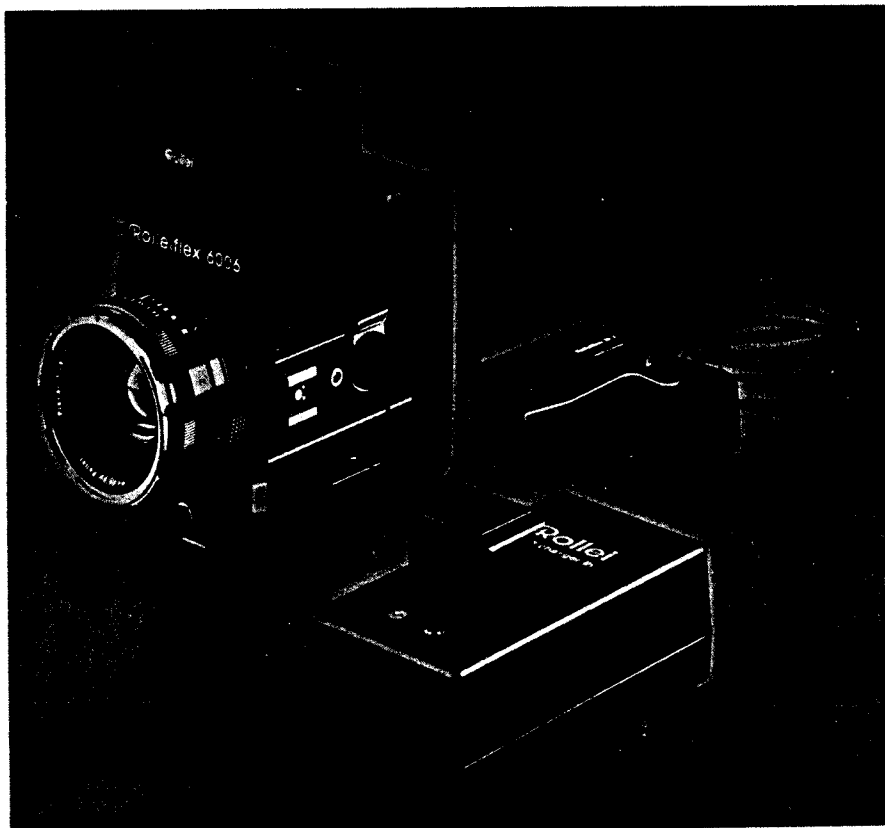
The term " analytical photogrammetry " is referred only to the data analysis and means, that all steps necessary are numerically carried out.

A first reconsideration of analytical photogrammetry represents a surveying method, which is very versatile and, moreover, archives the object state for inspections later on. Its main advantages are short times for taking the pictures, it does not get in contact with the object to be measured, and a large point manifold can be determined very economically.

- (a) WILD P31 metric camera (focal length $c \approx 100$ (mm), picture format 10 x 12 (cm))



(b) ROLLEI SLX semi-metric camera (focal length variabel, picture format 6 x 6 (cm))



(c) The monocomparator and analytical plotter principle

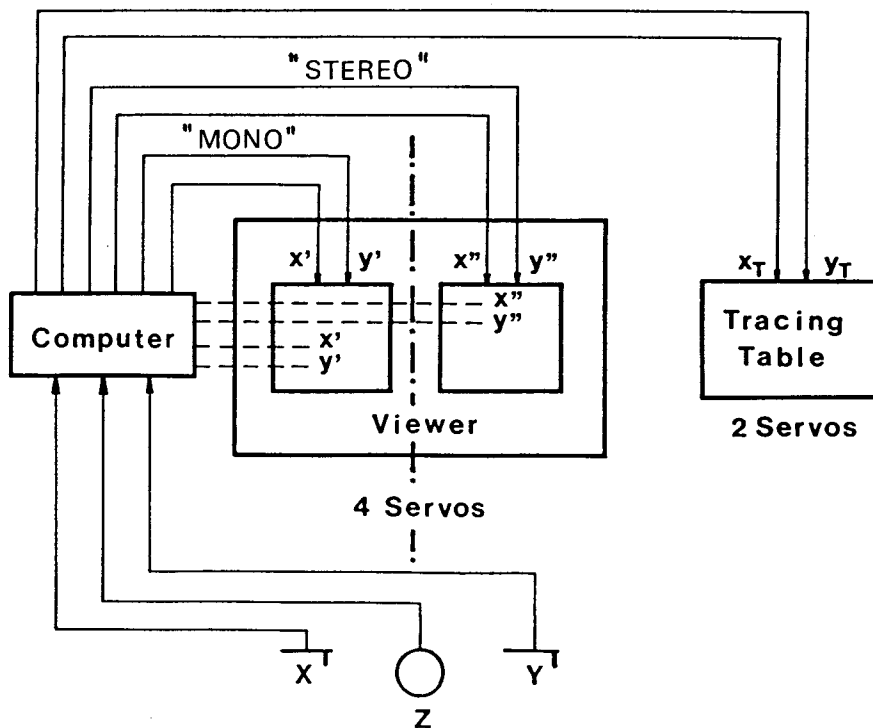


Fig. 2: Photogrammetric data acquisition equipment

3. Point Determination by Bundle Block Adjustment

The photogrammetric point determination goes back to the thirties, when it was used for radial triangulation and spatial aerial triangulation. For a long time it served mainly internal photogrammetric tasks namely for network densification to provide for control points. But since the sixties the progress in accuracy has been started influenced by better hardware (cameras, film, precise measurement equipment) and above all by the introduction of block adjustments. These developments made photogrammetry universal and reliable, so that today all precise point determinations are obtained by adjustment techniques. The principle of photogrammetric point determination by the most rigorous approach of the bundle method is demonstrated in Fig. 3.

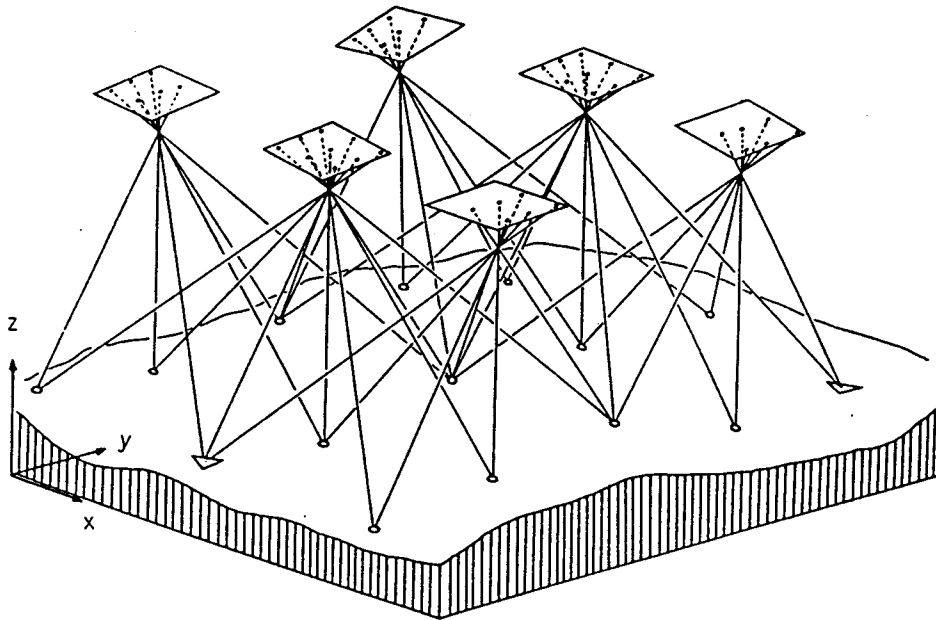


Fig. 3: Bundle method for photogrammetric point determination

Let us start from the central - perspective image transformation between the images (photograms) and the object space (K. Schwidersky / F. Ackermann, 1976)

$$\begin{bmatrix} x - x_i \\ y - y_i \\ -c \end{bmatrix} = sR \begin{bmatrix} X - X_i \\ Y - Y_i \\ Z - Z_i \end{bmatrix} \quad (1)$$

with $x_i, y_i \forall i=1,2, \dots$ as image coordinates of point P_i , c is the calibrated focal length, and x_0, y_0 are the coordinates of the principle point, in which the coordinate system of the image is centered; the right hand-side consists of a scale factor s , the rotation matrix R and the object coordinates X_i, Y_i, Z_i of P_i as well as the coordinates X_0, Y_0, Z_0 of the projection centre. If the scale factor s is resolved and substituted, the well-known observation functionals are obtained

$$\frac{x_i - x_0}{c} = - \frac{r_{11}(X_i - X_0) + r_{12}(Y_i - Y_0) + r_{13}(Z_i - Z_0)}{r_{31}(X_i - X_0) + r_{32}(Y_i - Y_0) + r_{33}(Z_i - Z_0)} \quad (2a)$$

$$\frac{y_i - y_0}{c} = - \frac{r_{21}(X_i - X_0) + r_{22}(Y_i - Y_0) + r_{23}(Z_i - Z_0)}{r_{31}(X_i - X_0) + r_{32}(Y_i - Y_0) + r_{33}(Z_i - Z_0)} \quad (2b)$$

For a fixed "interior orientation" of the camera, what means, that the coordinates of the principle point x_0, y_0 and the focal length c are known, the left-hand side can be interpreted as "angles" to be measured. As rotation matrix $R=(r_{ij}) \forall i,j=1,2,3$ may serve the Rodrigues representation $R=f(q_0, q_1, q_2, q_3)$ with the coordinates of a quaternion (E.W. Grafarend, 1983) or the traditionally one using sequential rotations by the Cardan axes φ, ω, κ

$$R = \begin{bmatrix} r_{11} & r_{12} & r_{13} \\ r_{21} & r_{22} & r_{23} \\ r_{31} & r_{32} & r_{33} \end{bmatrix} = R(\varphi)R(\omega)R(\kappa) \quad (3a)$$

with

$$R(\varphi) = \begin{bmatrix} 1 & 0 & 0 \\ 0 & \cos \varphi & \sin \varphi \\ 0 & -\sin \varphi & \cos \varphi \end{bmatrix}, \quad R(\omega) = \begin{bmatrix} \cos \omega & 0 & -\sin \omega \\ 0 & 1 & 0 \\ \sin \omega & 0 & \cos \omega \end{bmatrix}$$

$$R(\kappa) = \begin{bmatrix} \cos \kappa & \sin \kappa & 0 \\ -\sin \kappa & \cos \kappa & 0 \\ 0 & 0 & 1 \end{bmatrix} \quad (3b)$$

Thus the considerations above show, that photogrammetric point determination is nothing else than spatial triangulation. This means the photogrammetric network measured by angles is invariant against S-transformations within the \mathbb{R}^3 , so that the point manifold can be translated, rotated and scaled without changing the observations. The number of non-estimable parameters will be 7, i.e., 3 translations, 3 rotations and 1 scale factor, which define the datum of the triangulation.

In order to estimate the parameters of the "exterior orientation" $X, Y, Z, \varphi, \omega, \kappa$ as well as the object coordinates X_i, Y_i, Z_i by means of the observation functionals (2) this rank deficiency must be overcome. Traditionally the datum problem is solved by the introduction of coordinates of control points, whose number is greater than or equal the rank (datum) deficiency. The minimum requirements are 2 control points with full object information (X_C, Y_C, Z_C) and one control point in height (Z_C), but there are also other constellations admitted.

For the detection of displacements and in very precise applications the datum should not be fixed a priori; a better solution would be to do the datum transformation afterwards in any S-system to be defined (D. Fritsch, 1986). A further advantage is the unbiased estimation of the interior accuracy of the photogrammetric point determination, which is not disturbed by this approach.

After the linearization of (2) (K. Schwidersky/F. Ackermann, 1976) the unknown parameters are estimated by adjustment techniques leading to the concept of "bundle block adjustment". For that reason let us introduce the Gauss-Markov model not of full rank (K.R. Koch, 1987)

$$E(l) := l + v = \begin{bmatrix} A_1 & A_2 & A_3 \end{bmatrix} \begin{bmatrix} x_1 \\ x_2 \\ x_3 \end{bmatrix}, \quad D(l) = \sigma^2 p^{-1} \quad (4)$$

subject to $\begin{bmatrix} H \\ B \end{bmatrix} x = \begin{bmatrix} w \\ 0 \end{bmatrix}, \quad x := [x_1^1, x_2^1, x_3^1]^T$

in which the rx_1 vector x_1 contains the unknown coordinates $X_i, Y_i, Z_i \forall i=1,2,\dots,r$ of the object points; the exterior orientation parameters are represented by the sx_1 vector x_2 , and there is also room left for additional parameters by the tx_1 vector x_3 , for example to compensate film deformations and to use additional information on the object, respectively. The coefficient matrices A_1, A_2, A_3 contain the partial derivatives of the linearization process. E is the expectation which leads to a consistent formulation of the linear model by means of the introduction of an inconsistency or residual vector v to the observations l ; the accuracy level or dispersion D is given by an unknown variance factor of unit weight σ^2 and the corresponding positive definite matrix of

cofactors P^{-1} .

Restrictions on the parameter estimation are considered with $Hx=w$, if general requirements such as known distances between some object points have to be fulfilled; the datum deficiency is overcome by means of $Bx=0$ (D. Fritsch et al., 1984). In order to have minimum variances for the coordinates of object points, the datum deficiency is removed with the formulation

$$\boxed{x_1^i x_1} = \min \quad (5)$$

i.e., the matrix B should cause (differential) changes only with regard to these parameters (D. Fritsch/B. Schaffrin, 1982). With $B:=(B_1, B_2, B_3)$ it follows $B_2=B_3=0$ and

$$B_1 = \begin{bmatrix} 1 & 0 & 0 & 1 & 0 & 0 \\ 0 & 1 & 0 & 0 & 1 & 0 & \dots & \text{"transl."} \\ 0 & 0 & 1 & 0 & 0 & 1 & & \\ \hline 0 & -Z & Y & 0 & -Z & Y & & \\ & 1\sigma & 1\sigma & & 2\sigma & 2\sigma & & \\ Z & 0 & -X & Z & 0 & -X & \dots & \text{"rotat."} \\ 1\sigma & & 1\sigma & 2\sigma & & 2\sigma & & \\ -Y & X & 0 & -Y & X & 0 & & \\ \hline 1\sigma & 1\sigma & & 2\sigma & 2\sigma & & & \\ X & Y & Z & X & Y & Z & \dots & \text{"scale"} \\ 1\sigma & 1\sigma & 1\sigma & 2\sigma & 2\sigma & 2\sigma & & \end{bmatrix} \quad (6)$$

if a rank deficiency $u-q=7$ is supposed; the coefficients X_{i0}, Y_{i0}, Z_{i0} are approximate coordinates of the object points to be used for the rotations and the scale of the triangulation.

The objective function of least squares

$$v^i P v = \min \quad \text{subject to} \quad \begin{bmatrix} H \\ B \end{bmatrix} x = \begin{bmatrix} w \\ 0 \end{bmatrix} \quad (7)$$

leads with $N := A^i P A$ as well as $b := A^i P l$ to the normal equations

$$\begin{bmatrix} N & & & H^i & B^i \\ 11 & 12 & 13 & 1 & 1 \\ N & N & N & H^i & 0 \\ 21 & 22 & 23 & 2 & 0 \\ N & N & N & H^i & 0 \\ 31 & 32 & 33 & 3 & 0 \\ H & H & H & 0 & 0 \\ 1 & 2 & 3 & 0 & 0 \\ B & 0 & 0 & 0 & 0 \\ 1 & & & & \end{bmatrix} \begin{bmatrix} \hat{x} \\ \hat{x}_1 \\ \hat{x}_2 \\ \hat{x}_3 \\ \hat{\lambda}_h \\ \hat{\lambda}_b \end{bmatrix} = \begin{bmatrix} b \\ b_1 \\ b_2 \\ b_3 \\ w \\ 0 \end{bmatrix} \quad (8)$$

which may be solved by means of pivot strategies and efficient formulas (K.R. Koch, 1987), respectively.

Another, more operational procedure, considers the restrictions as observations with infinite accuracy to be solved by setting their weights $p_i \gg 1$. This approach is realized in most of the programme packages available for bundle block adjustment. Also the datum problem is pragmatically overcome such that the coordinates of control points are considered as random observations with corresponding accuracy measures. Software packages exist at least at the university level, but may be purchased from photogrammetric institutes and private companies, too. These packages are very comprehensive and are capable to solve thousands of unknown parameters simultaneously such as PAT-B, Stuttgart, BINGO, Hannover / Oberkochen, MOR-S, Bonn/Braunschweig, CLIC, Munich, to name some programmes developed in the Federal Republic of Germany.

4. Model Building and Hypothesis Testing

In order to detect movements between different time epochs by means of photogrammetric point determination the model (4) must be extended and supplemented by hypothesis testing. For that reason, the following models will consider the requirements of modern parameter estimation. The model building is restricted to be static and not kinematic between the exposure epochs. Furthermore, for reasons of simplicity only models for pairwise different epochs will be given.

(i) Let us generalize the model (4) by a further observation epoch and define

$$E(l_{ij}) := E \begin{pmatrix} 1 \\ i \\ 1 \\ j \end{pmatrix} = \begin{bmatrix} Z_i & 0 \\ 0 & Z_j \end{bmatrix} \begin{pmatrix} x_i \\ x_j \end{pmatrix} =: Z_{ij} x_{ij} \quad (9a)$$

$$D(l_{ij}) := D \begin{pmatrix} 1 \\ i \\ 1 \\ j \end{pmatrix} = \begin{bmatrix} \sigma_i^2 P^{-1} & 0 \\ 0 & \sigma_j^2 P^{-1} \end{bmatrix} \quad (9b)$$

which we will call a " sequential " Gauss-Markov model; according to (4) the coefficient matrix Z_k and the vector $x_k \forall k=i,j$ are substitutes for

$$Z_k := [A_1, A_2, A_3] \quad (10a)$$

$$x_k := [x_1^i, x_2^i, x_3^i]' \quad (10b)$$

The general solution by least squares leads to partly MINOLESS-type

estimates (Minimum Norm Least Squares Solution, B. Schaffrin, 1975, K.R. Koch, 1987)

$$\hat{x}_k = (Z^T P_k Z)^{-1} Z^T P_k l_k \quad (11a)$$

$$D(\hat{x}_k) = \sigma_k^2 (Z^T P_k Z)^{-1} \quad (11b)$$

$$\hat{\sigma}_k^2 = \hat{v}_k^T P_k \hat{v}_k / (n_k - q_k) \quad (11c)$$

(ii) In order to detect displacements more sensitive K.R. Koch (1983, 1987) proposes the following model

$$E(l_{ij}) := E\left(\begin{bmatrix} l_i \\ l_j \end{bmatrix}\right) = \begin{bmatrix} Z & 0 \\ 0 & Z \end{bmatrix} \begin{bmatrix} x_i \\ x_j \end{bmatrix} =: \begin{bmatrix} Z & x_{ij} \\ & Z \end{bmatrix} \quad (12a)$$

$$D(l_{ij}) := D\left(\begin{bmatrix} l_i \\ l_j \end{bmatrix}\right) = \begin{bmatrix} \sigma_i^2 P_i^{-1} & \sigma_{ij} P_{ij}^{-1} \\ \sigma_{ij} P_{ij}^{-1} & \sigma_j^2 P_j^{-1} \end{bmatrix} \quad (12b)$$

it is called "multivariate" Gauss-Markov model. The $n \times u$ coefficient matrix Z must be the same for every exposure epoch, the same holds for the weight matrix P but with the advantage of estimating the covariance component between the epochs i and j . This covariance component is a number for homogeneous data acquisition in both observation epochs; i.e. the same exposure disposition, the same region being controlled, the same device for obtaining the image coordinates, and so on.

Applying the partly MINOLESS estimate within the multivariate Gauss-Markov model results to

$$\hat{x}_k = (Z^T P_k Z)^{-1} Z^T P_k l_k \quad (13a)$$

$$D(\hat{x}_k) = \sigma_k^2 (Z^T P_k Z)^{-1} \quad \forall k=i, j \quad (13b)$$

and, moreover, gives the estimates for the variances and covariances by

$$\hat{\sigma}_k^2 = \hat{v}_k^T P_k \hat{v}_k / (n_k - q_k) \quad (14a)$$

$$\hat{\sigma}_{ij}^2 = \hat{V}_i^T P V_j / (n - q) \quad (14b)$$

The estimated parameters \hat{x} are independent of the covariance component σ_{ij}^2 .

For separation of the set of control points and object points into two disjunctive sets of fixed points and variable points, hypotheses will be introduced. Because of the different models, hypotheses testing methods will differ somewhat from each other, as can be seen in the following.

(i) The hypothesis test within the sequential Gauss-Markov model presupposes any test on homogeneity of the observations between the two epochs; this can be stated as follows:

$$H_0: \sigma_i^2 = \sigma_j^2 \text{ against } H_1: \sigma_i^2 \neq \sigma_j^2 \quad (15)$$

its acceptance or rejection depends on the variance ratio (H. Wolf, 1975)

$$\sigma_i^2 / \sigma_j^2 \sim F(u_i - q, u_j - q) \quad (16)$$

If the hypothesis (15) has been accepted one can proceed with formulations on hypothesis testing for point movements or on deviations of known parametric object models. For this reason, let us introduce the hypothesis:

$$H_0: |x_{1i}^{(P_i)} - x_{1j}^{(P_i)}| = 0 \text{ against } H_1: |x_{1i}^{(P_i)} - x_{1j}^{(P_i)}| \neq 0 \quad (17)$$

for pointwise hypothesis testing, in which individual coordinates or all coordinates of point P_i can be tested. Its corresponding test statistic is given by K.R. Koch (1985):

$$T = \frac{1}{r(\hat{\sigma}_i^2 + \hat{\sigma}_j^2)} \left(\hat{x}_{1i}^{(P_i)} - \hat{x}_{1j}^{(P_i)} \right)^T \left[\left((Z_i^T P_i Z_i)^{-1} \right) + \left((Z_j^T P_j Z_j)^{-1} \right) \right]^{-1} \left(\hat{x}_{1i}^{(P_i)} - \hat{x}_{1j}^{(P_i)} \right) \quad (18)$$

and decides on acceptance if $T < F_{1-\alpha; r, n_{ij} - q_{ij}}$ or the percentage point

$$\alpha_T = \int_T^\infty F(r, n_{ij} - q_{ij}) dT > \alpha \quad (19)$$

Both test values are depending on the number of hypotheses r .
(ii) Let hypotheses (17) within the multivariate Gauss-Markov model be defined. The following test value decides on acceptance or rejection:

$$T = \frac{1}{r(\hat{\sigma}_i^2 - 2\hat{\sigma}_{ij} + \hat{\sigma}_j^2)} \left(\hat{x}^{(P_i)} - \hat{x}^{(P_j)} \right)' \left((Z'PZ)^{-1} \right) \left(\hat{x}^{(P_i)} - \hat{x}^{(P_j)} \right) \quad (20)$$

which considers the covariance between epoch i and epoch j .

5. Examples

For demonstration of the efficiency of the photogrammetric point determination two examples are presented.

(i) Let us consider an example coming from brown-coal mining, where an area of opencast mining has been controlled for movements caused by working of the coal. The area contains many control points and additional points, which we will call quality points, determined by classical geodetic measurements with an accuracy of about $\sigma_{x,y} = \pm 10$ (mm). From these points a quality control of the photogrammetric point determination should be derived. The observation scheme of aerial positioning of the camera is given in Fig. 4.

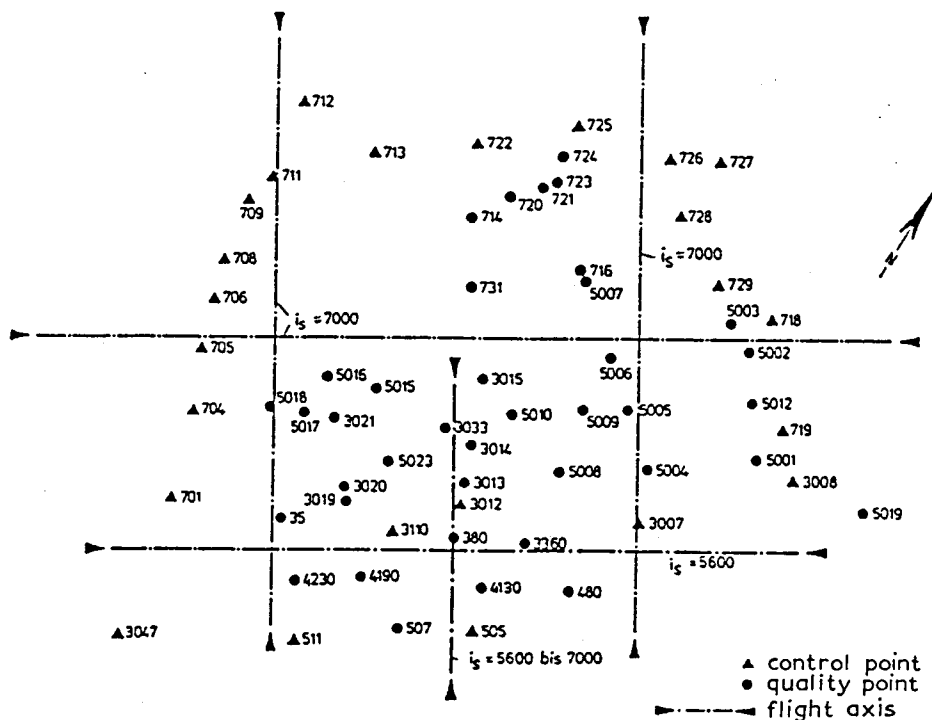


Fig. 4: Observation scheme and control points

All control points and quality points geodetically determined have been signalized for precise photogrammetric evaluation. The whole area is flown periodically since 1978 (K. Reichenbach, 1981), but let us consider only two photogrammetric evaluations for demonstrating the accuracies being achieved (see Table 1 and 2).

Table 1: Information on exposures and image evaluations

Date of exposure	Image scale	Camera	Comparator	Evaluation programme
1.11.80	7000 5600	Zeiss 15/23 AIV	Zeiss PSK 1	PAT-B* with self calibration
16.11.81	7000 5600	Zeiss 15/23 AIV	Zeiss PSK 1	PAT-B* with self calibration

*Bundle Adjustment within sequential Gauss-Markov models with control points as random informations and additional parameters for the compensation of systematic errors.

The values $\hat{\sigma}_x$ and $\hat{\sigma}_y$ demonstrate rms-deviations for control points and quality points between geodetic and photogrammetric point determination, whereby $\hat{\epsilon}_{xmax}$ and $\hat{\epsilon}_{ymax}$ are numbers for maximum deviations of control points only. The interior accuracy of the photogrammetric point determination can be given to

$$5.4 \text{ (mm)} \leq \hat{\sigma}_x, \hat{\sigma}_y \leq 16.5 \text{ (mm)}$$

with $\hat{\sigma}_{rms} = +7.9 \text{ (mm)}$ (Deutsch. Braunkohlen-Industrie-Verein e.V., 1983).

Table 2: Absolute accuracies

Date of exposure	Point type	$\hat{\sigma}$ (μm)	$\hat{\sigma}_x$ (mm)	$\hat{\sigma}_y$ (mm)	$\hat{\epsilon}_{xmax}$ (mm)	$\hat{\epsilon}_{ymax}$ (mm)
1.11.80	control	3.4	11	10	-	-
	quality		12	19	28	38
16.11.81	control	3.4	6	10	-	-
	quality		6	10	15	20

For a demonstration of hypothesis testing, let us take same samples of the point manifold determined photogrammetrically. Because of the availability of variances, the tests are restricted to single coordinates only and not groups of coordinates. The test on homogeneity delivers $\hat{\sigma}_1^2/\hat{\sigma}_2^2 = 1.0$ and will be accepted for redundancy $f=1250$ and $\alpha=0.05$. The points tested with its corresponding test values are represented in Table 3.

As we can see from Table 3, for example, it is not allowed to use the x,y-coordinates of point 713 as random observation for datum's defini-

tion in the bundle block adjustment.

Table 3: Hypothesis test for $\hat{\sigma}_{x,y} = \pm 8$ (mm) and $\hat{\sigma}_z = \pm 16$ (mm)

Point	Coordinates	T	Movements ($\alpha=0.05$)	
			Yes	No
713	x	1.56	*	
	y	6.25	*	
	z	0		*
3015	x	0.19		*
	y	4.25	*	
	z	151.6	*	
3021	x	3.29	*	
	y	0.06		*
	z	1.00		*

Therefore, it is indispensable to check the control information, in particular in moving areas, to introduce only fix points to overcome the rank deficiency. Moreover, variable points can be found by this approach to make final assertions on movements within the region being controlled.

(ii) In order to reconstruct a subreflector - part of an antenna system for satellite communications - its surface has been signalized for high precise photogrammetric point determination. The reflector is to describe by a hyperboloid of a diameter of about 2 (m) with ≈ 0.65 (m) in height. Its contour consists of aluminium sheet, for which maximum deviations of 0.3 (mm) are allowed within the inner range; the outer area may have maximum deviations of about 0.5 (mm).

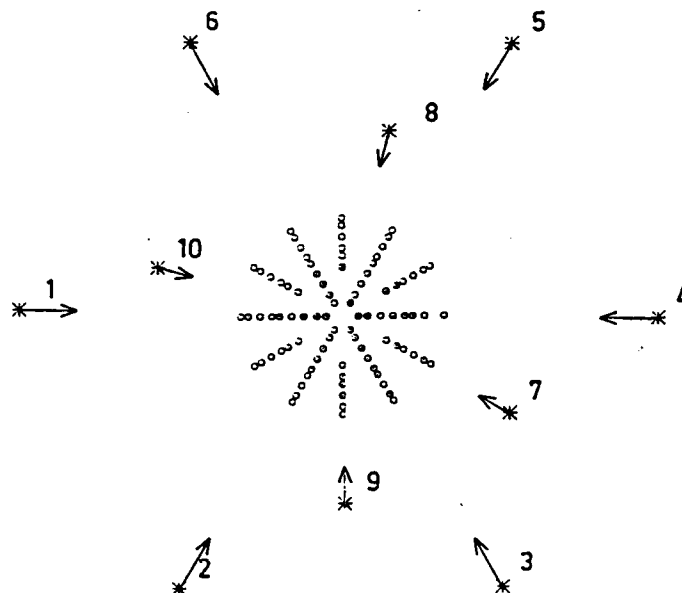


Fig. 5: Photogrammetric disposition for surveying of the subreflector

The photographs have been taken by the metric camera WILD P31 with calibrated focal length $c=99.56$ (mm) and an additional intermediate ring of $\Delta c=+3.78$ (mm) to provide for short distances. Glas plates of format 102×127 (mm) were preferred as carrier for the emulsion because of its stable behaviour against systematic errors. In Fig. 5 the photogrammetric disposition is presented: the exposures from the planar points $1, 2, \dots, 6$ ($\varphi \approx 0$ (Grad)) have been supplemented by four photographs with $\varphi \approx -50$ (Grad) (points 7, 8, 9, 10) to have a stable geometry of the bundle block. The Fig. 6 and 7 demonstrate photographs for this disposition its scale varies from about 1:30 to 1:20.

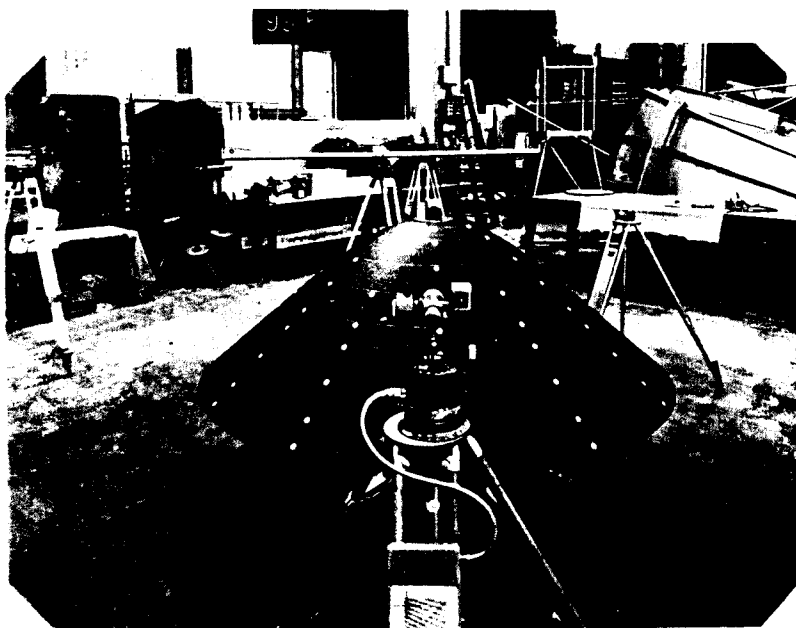


Fig. 6: Horizontal exposure



Fig. 7: Tilted exposure

For the measurement of the image coordinates the monocomparator Zeiss PSK 1 have been used. A first estimation of its accuracy a priori delivered $\hat{\sigma}_x = \pm 0.0015$ (mm) and $\hat{\sigma}_y = \pm 0.0018$ (mm). The bundle block adjustment by means of the CLIC - package gave the following accuracy measures for the coordinates of the 90 object points

$$\hat{\sigma}_x = \pm 0.053 \text{ (mm)} , \quad \hat{\sigma}_y = \pm 0.054 \text{ (mm)} , \quad \hat{\sigma}_z = \pm 0.057 \text{ (mm)}$$

These figures are in full accordance with a classical geodetic point determination by means of theodolite and a 2 (m) distance batten (D. Fritsch et al., 1984).

Using the information on the shape of the reflector will probably provide for better accuracy figures.

6. New Developments and Conclusions

With the development of digital vision sensors the disadvantage of analog photographs can be overcome. This means, that all the operations demonstrated in Fig. 1 can be handled purely digitally producing an automated data flow from data capturing to object reconstruction. For that reason photogrammetric point determination becomes once more attractive, especially in close range applications (D. Fritsch/G. Strunz, 1987). There are some advantages of these new sensors characterized by Charge Coupled Devices (CCD), Charge Injection Devices (CID) or Photodiodes; first of all they deliver a digital picture (digigram) of the object to be controlled. A typical example of a CCD - camera is given by Fig.8.

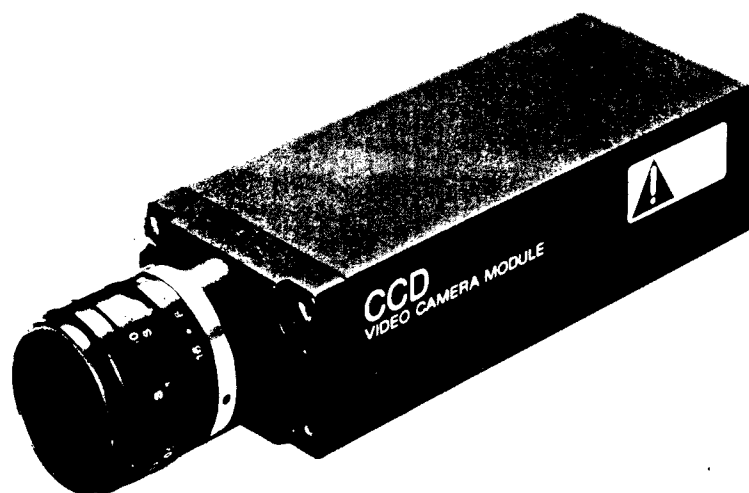


Fig. 8: Solid state CCD - camera with 756 H x 581 V elements, square pixel size of 11.0 x 11.0 μm , compact size & light weight

As shown by the examples above, photogrammetry today is a very efficient surveying method. Although it is in rivalry with electronic theodolites and other surveying equipment, these new developments can also integrate photogrammetric methods into classical measurement techniques and vice versa. A recent product of KERN, Switzerland, makes use of bundle block adjustment for the evaluation of the data of the "SPACE" system (R. Gottwald, W. Berner, 1987) - System for Positioning and Automatic Coordinate Evaluation - , in which a CCD - sensor is installed inside an electronic theodolite. This leads to a new generation of "photo theodolites" (see Fig. 9) as efficient systems for an automated object monitoring and for the detection of displacements. Thus, new fields are open for photogrammetric methods - a challenge to be accepted by every surveyor. Last not least the bundle block adjustment contributed a lot to this progress.

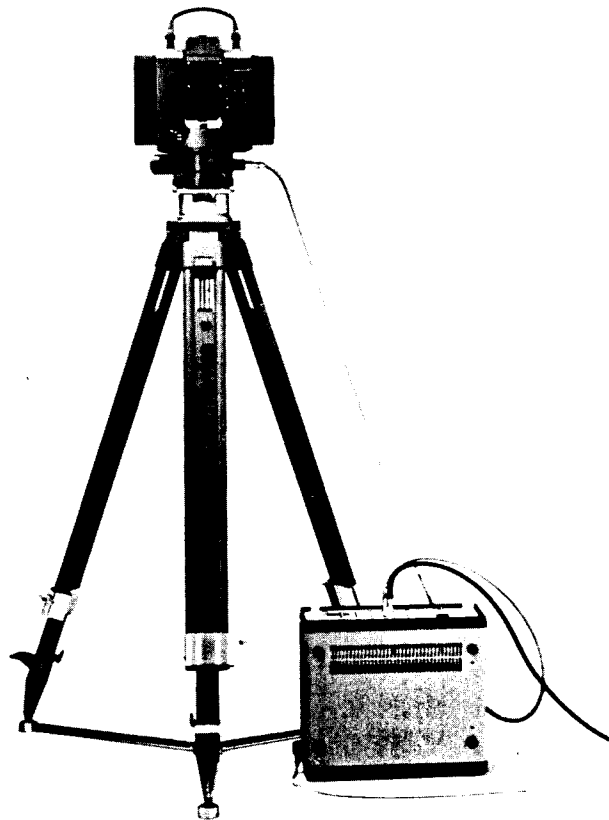


Fig. 9: A new type of " photo-theodolite "

REFERENCES

- DEUTSCHER BRAUNKOHLLEN - INDUSTRIE - VEREIN e.V. (1983): Messung von Böschungsbewegungen in Braunkohletagebauen. Abschlussbericht, Köln.
- EBNER, H. (1981): The Analytical Plotter and Numerical Photogrammetry. Photogrammetric Record, 10, pp. 409-420.
- FRITSCH, D./B. SCHAFFRIN (1982): The 'Choice of Norm' Problem for the Free Net Adjustment with Orientation Parameters. Boll. Geod. Scien. Aff., 41, pp. 259-282.
- FRITSCH, D./H. KLENNERT/F. MÜLLER/R. REISER/M. STEPHANI (1984): Hochpräzise photogrammetrische Vermessung von Industrieobjekten. In: Ingenieurvermessung 84, Ed. K. Rinner/G. Schelling/G. Brandstätter, Dümmler, Bonn, 2, C9.
- FRITSCH, D. (1986): Photogrammetry as a Tool for Detecting Recent Crustal Movements. Tectonophysics, 130, pp. 407-420.
- FRITSCH, D./G. STRUNZ (1987): Automatic Digital Reconstruction of Simple Objects by Advanced Photogrammetric Methods. Pres. Pap. 41. Photogrammetric Week, Inst. Photogr., Stuttgart Univ., Stuttgart.
- GOTTWALD, R./W. BERNER (1987): Electronic Theodolites - Sensor-Systems for Real-Time Photogrammetry? Proceed. Intercomm. Conf. Fast Process. Photogr. Data, Eidgen. Techn. Hochsch., Inst. Geod., Photogr., Zurich
- GRAFAREND, E.W. (1983): Stochastic Models for Point Manifolds. Deutsche Geod. Komm., Reihe A, 98, pp. 29-52.
- HELAVA, U.V. (1957): New Principle for Photogrammetric Plotters. Photogrammetria, 14, pp. 89-96.
- KOCH, K.R. (1983): Estimation of Variances and Covariances in the Multivariate and in the Incomplete Multivariate Model. Deutsche Geod. Komm., Reihe A, 98, pp. 53-59.
- KOCH, K.R. (1985): Ein statistisches Auswerteverfahren für Deformationsmessungen. Allgem. Verm. Nachr., 92, pp. 97-108.
- KOCH, K.R. (1987): Parameterschätzung und Hypothesentests. 2. Aufl., Dümmler, Bonn.
- REICHENBACH, K. (1981): Zur Genauigkeit der aerophotogrammetrischen Punktbestimmung. Das Markscheidewesen, 88(2).
- SCHAFFRIN, B. (1975): Zur Verzerrtheit von Ausgleichungsergebnissen. Mitt. Inst. Theor. Geod., Univ. Bonn, 39.
- SCHMID, H.H. (1956): An Analytical Treatment of the Problem of Triangulation by Stereophotogrammetry. Photogrammetria, 13, pp. 67-77.
- SCHWIDEFSKY, K. / F. ACKERMANN (1976): Photogrammetrie. B.G. Teubner, Stuttgart.

- STEPHANI, M. / K. EDER (1987): Leistungspotential einer Teilmesskammer beim Einsatz in der Architekturphotogrammetrie. Bildmess., Luftbildwes. (BuL), 55, pp. 204-213.
- WESTER-EBBINGHAUS, W. (1983): Ein photogrammetrisches System für Sonderanwendungen. Bildmess., Luftbildwes., (BuL), 51, pp. 118-128.
- WOLF, H. (1975): Ausgleichsrechnung, Dümmler, Bonn.